Case Report
J Vet Intern Med 2014;28:1881–1885

Cerebral High-grade Oligodendroglioma with Sarcomatous Transdifferentiation ("Oligosarcoma") in a Boxer Dog

A. Fadda, I. Vajtai, J. Lang, D. Henke, and A. Oevermann

Key words: Glial tumors; Primary canine intracranial tumor.

A 9-year-old female spayed boxer was referred to the Veterinary Teaching Hospital of the University of Bern for a history of chronic neck pain and neurologic deficits. One month before presentation, the dog had been treated with carprofen[a] (2 mg/kg once daily) and ordered restriction of exercise. Clinical signs improved transiently but, 1 week before presentation, the dog relapsed despite continued treatment and manifested severe cervical pain and gait problems, which rapidly progressed to a nonambulatory status. Physical examination was noncontributory. Neurologic examination revealed obtunded mentation along with a nonambulatory tetraparesis. Postural reactions were decreased to absent in all four limbs, while segmental spinal reflexes persisted intact. There were bilaterally reduced menace responses and a spontaneous vertical nystagmus. Passive lateral and dorsal flexion of the neck elicited a pain response. The neurologic status was deemed to be consistent with a multifocal process in the forebrain, brainstem, and cervical spinal cord (C1–C5), possibly involving the meninges as well. At this stage, differential diagnoses included both neoplastic and inflammatory diseases with multifocal involvement. A complete blood cell count, serum biochemistry profile, plasma ammonia concentration, fasting and postprandial bile acids, T4 and TSH levels were all within reference ranges. Chest radiographs were unremarkable.

Magnetic resonance imaging (MRI) of the head and neck was performed using a 1 Tesla Panorama HFO from Philips under general anesthesia. Anesthesia was induced with fentanyl[b] (5 μg/kg IV) and propofol[c] (4 mg/kg IV). This included T2-weighted (T2W) sequences in sagittal and transverse planes, fluid-attenuated inversion recovery (FLAIR) sequences in dorsal and transverse planes, dorsal and transverse T1W pre- and postcontrast sequences, and transverse T2*-weighted (T2W) gradient echo sequences. Scans revealed a large left-sided, intra-axial space-occupying lesion that was divided into two portions interconnected by a thin isthmus at the level of the cerebellar tentorium (Fig 1A,B). The mass was surrounded by extensive perilesional edema (Fig 1A). The larger rostral portion was located ventrolaterally in the cranial fossa, and extended from the frontal to the piriform lobe; the smaller portion was located laterally in the caudal fossa above the petrous bone. The rostral portion of the mass caused midline shift to the right, displacing and attenuating the ventral aspect of the left lateral ventricle. In transverse sections, it was moderately delineated and contained T2-hyperintense (Fig 1C), and T1-hypointense cavities that showed incomplete suppression on FLAIR sequences. After contrast administration, the ventral cavitary lesion appeared delineated by a contrast-enhancing rim (Fig 1D). An area with more heterogeneous contrast enhancement was located rostral to the cavity (Fig 1B). The mass extended into the meninges at the ventral margins of the piriform lobe and basal nuclei (Fig 1C,D), where it showed strong and homogeneous contrast enhancement (Fig 1D). No evidence of hemorrhage was found on T2* sequences. The caudal, subtentorial portion of the mass was hypointense in T1W and hyperintense in T2W images. In transverse sections, it appeared to be predominantly extra-axial and shared similar MRI characteristics with the rostral portion (Fig 1E,F). Mild hydrocephalus and hydrosyringomyelia of the first cervical segments of the spinal cord were observed. Mild mucosal thickening with mild contrast enhancement was observed in the left bulla. Further diagnostic evaluation, including a stereotactic brain biopsy, was declined by the owner. The dog was euthanized at the owner's request, and permission was granted to perform necropsy (Figs 2, 3).

Gross examination of the brain revealed a round, grayish, ill-defined mass with soft to gelatinous consistency in the left piriform and temporal lobe, causing midline shift to the right. The mass abutted on the left lateral ventricle, and extended to the meninges at the base of the skull. The center of the mass was cystic. The macroscopic appearance of the lesion in the caudal fossa was similar. Histologic examination revealed a biphasic tumor composed of alternating neuroepithelial and mesenchymal cell populations. The former displayed characteristics of conventional anaplastic oligodendroglioma (WHO grade III). Dispersed on a mucinous background, tumor cells exhibited roundish,

From the Division of Neurological Sciences, Department of Clinical Veterinary Medicine, Vetsuisse Faculty, (Fadda); the Section of Neuropathology, Institute of Pathology, (Vajtai); the Division of Clinical Radiology, Department of Clinical Veterinary Medicine, Vetsuisse Faculty, (Lang); and the Department of Clinical Research and Veterinary Public Health, University of Bern, Berne, Switzerland (Henke, Oevermann).

Preliminary data of this case report were previously presented as poster presentation at the 26th ECVN/ESVN Annual Symposium in Paris, France, 26–28 September 2013.

Corresponding author: A. Fadda, DVM, Division of Neurological Sciences, Department of Clinical Veterinary Medicine, Vetsuisse Faculty, University of Berne, Länggassstrasse n. 124, 3012 Berne, Switzerland; e-mail: angela.fadda@vetsuisse.unibe.ch.

Submitted May 13, 2014; Revised July 10, 2014; Accepted August 13, 2014.

DOI: 10.1111/jvim.12457

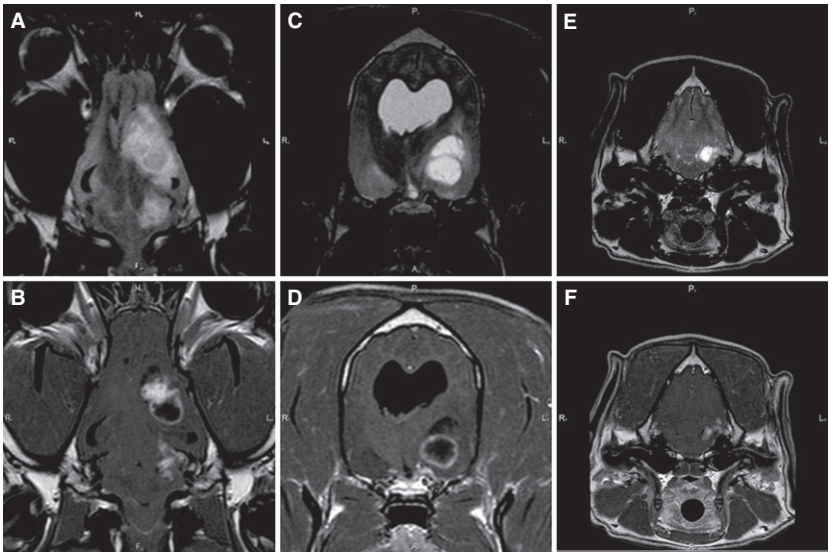

Fig 1. **(A)** Dorsal FLAIR image at the level of the orbits, showing the large left-sided, intra-axial space-occupying lesion extending from the cranial to the caudal fossa with extensive perilesional edema and incomplete suppression of the center of the cystic cavities. **(B)** Dorsal T1-weighted image after gadolinium administration at the level of the orbits, showing the rostral and caudal portion of the lesion connected by a thin isthmus at the height of the cerebellar tentorium. **(C)** Transverse T2W image and **(D)** transverse T1W image after gadolinium administration showing rim-like contrast enhancement of the rostral portion of the lesion, and strong and homogeneous contrast enhancement of the meningeal infiltration at the ventral margins of the piriform lobe and basal nucleus. **(E)** Transverse T2W image and **(F)** transverse T1W image after gadolinium administration of the subtentorial portion of the mass showing characteristics similar to the rostral portion.

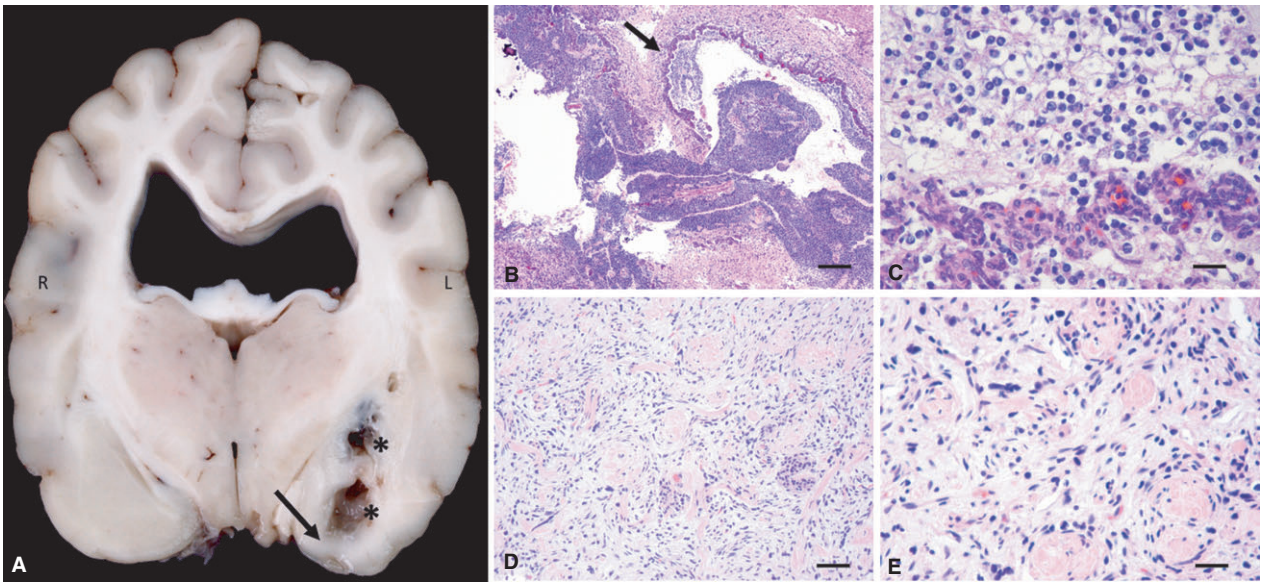

Fig 2. **(A)** Frontal slice through the formalin fixed the brain at necropsy showing an ill-defined mass in the left piriform and temporal lobe with multiple cystic cavities (asterisk). The mass has contact with the basal meninges (arrow). **(B, C)** Photomicrographs of the oligodendroglioma portion of the tumor, showing (B) a central cavity surrounded by a layer of neoplastic cells and microvascular proliferation (arrow) (H&E, 20×) (scale bar = 5 mm); (C) classical honeycomb pattern of neoplastic cells encased by glomeruloid microvascular structures (H&E, 200×) (scale bar = 50 μm); **(D)** (scale bar = 1000 μm). Photomicrographs of the sarcomatous portion in the subarachnoid space showing **(E)** (scale bar = 50 μm) fascicles of spindle cells separated by broad bands of collagen (H&E, 100× and 200×).

nonfibrillary cytoplasmic contours, mildly irregular hyperchromatic nuclei, and conspicuous perinuclear vacuolation producing an overall honeycomb-like texture. In between, several mucus-filled cysts were seen. The tumor's vasculature included both "chicken-wire" type capillaries and complex festoons of glomeruloid

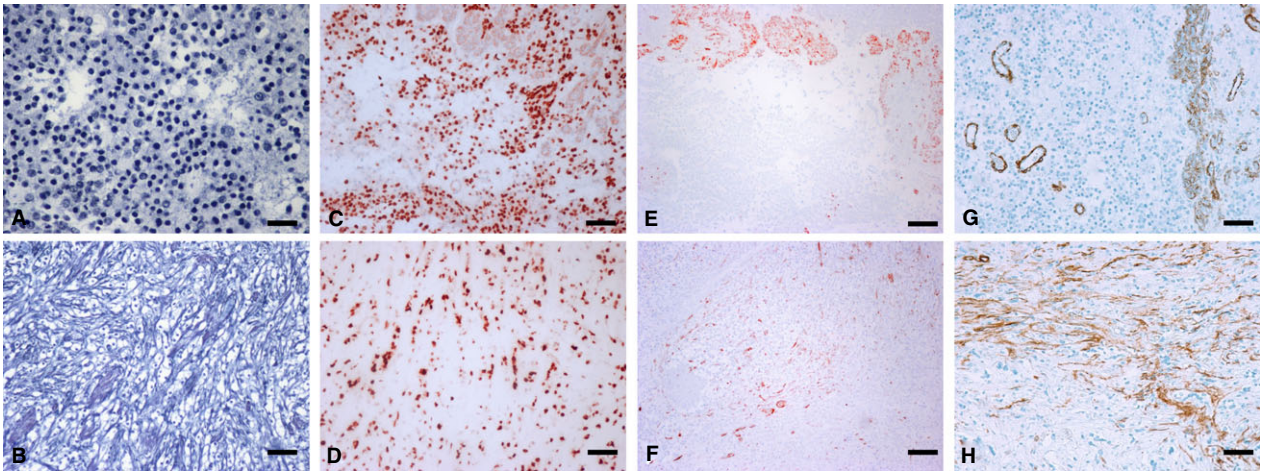

Fig 3. **(A)** Neoplastic cells of the conventional oligodendroglioma portion lack a pericellular basal membrane (Gomori's silver stain, 400×) (scale bar = 50 μm). **(B)** Neoplastic cells of the sarcomatous portion are surrounded by a pericellular basal membrane (Gomori's silver stain, 400×) (scale bar = 50 μm). **(C, D)** Nuclear anti-Olig2 positivity in neoplastic cells of both the oligodendroglial (C) and sarcomatous (D) portion (anti-Olig2 immunohistochemistry, 200×) (scale bar = 100 μm). **(E, F)** Immunohistochemistry for vimentin. In the oligodendroglial portion (E), vimentin is only expressed by microvascular structures, whereas neoplastic oligodendrocytes lack expression (100×); in the sarcomatous portion, neoplastic cells multifocally expressed vimentin (F, 100×). **(G, H)** Immunohistochemistry for smooth muscle actin (SMA). Similar to vimentin, in the oligodendroglial portion SMA is expressed by microvascular proliferations and intraneoplastic vessels only (G), whereas in the sarcomatous portion (H), SMA is multifocally expressed by neoplastic cells (125×) (scale bar = 100 μm). [Color figure can be viewed in the online issue, which is available at wileyonlinelibrary.com.]

proliferations. Up to 2 mitoses per 1 high-power field (HPF) were observed. Infiltrative growth was evident, as were "secondary structures of Scherer" around vessels and neurons. A pericellular basal lamina was not present after staining with Gomori's silver stain. Conversely, the mesenchymal population was characterized by haphazard fascicles of spindle cells on a mucinous matrix and amidst an intricate mesh of Gomori-impregnated pericellular basal lamina as well as broad bands of collagen. Here up to 3 mitoses per 1 HPF were observed. This portion of the tumor encroached upon the subarachnoid space around the optic chiasm and pituitary gland.

On immunohistochemistry, both tumor cell populations showed nuclear expression of Olig2.[d] Staining for glial fibrillary acidic protein (GFAP) (GFAP polyclonal[e]) tended to be restricted to interspersed reactive astrocytes within the oligodendroglial component, whereas some 5% of neoplastic spindle cells in the sarcomatous areas were positive. In addition, neoplastic cells in the sarcomatous but not the oligodendroglial areas focally expressed vimentin (Vimentin clone Vim3B4[e]), muscular actin (Muscle actin clone HHF35[e]), and smooth muscle actin,[f] but not S100 (S100 polyclonal and Desmin clone D33[e]) protein. Irrespective of architectural variations, the Ki-67 (MIB-1; Ki 67 clone MIB1[e]) labeling index averaged 5%. Based on the above findings, the tumor was diagnosed as anaplastic oligodendroglioma with heterologous sarcoma-like differentiation ("oligosarcoma").

Discussion

Glial tumors are the second most common primary intracranial neoplasm in dogs, and account for 35% of neuroepithelial tumors.[1] The two most common clinical signs associated with primary intracranial tumors of dogs located in the telencephalon are seizures and altered mentation.[1] In contrast, the dog described in this report was presented initially with severe neck pain. This might have been because of hydrosyringomyelia of the first cervical segments, which has been associated with persistent neuropathic pain in other breeds.[2,3]

Based on histologic similarities to human CNS tumors, the 2007 World Health Organization (WHO) classification system of human CNS tumors has been tentatively applied to the taxonomy and grading of various canine CNS tumors.[4–8] With the exception of a conspicuous oligodendroglial—rather than astrocytic—background, the microscopic and immunohistochemical features of the tumor described were consistent with a diagnosis of gliosarcoma, the latter being defined as "a glioblastoma variant characterized by a biphasic tissue pattern with alternating areas displaying glial and mesenchymal differentiation".[9] The glial moiety of gliosarcomas per definitionem involves astrocytic differentiation.[4–10] Alternatively, the descriptive labels "oligosarcoma" and "ependymosarcoma" have been proposed to accommodate those hybrid neuroepithelial-sarcomatous malignancies—exceedingly rare as a group—wherein the glioma component exhibits either oligodendrocytic or ependymal phenotype, respectively.[9,11–13] In our case, the anaplastic oligodendroglial element (WHO grade III) was diagnosed based on the presence of a monomorphous population of round cells with hyperchromatic nuclei strongly staining with Olig-2, honeycomb texture, microvascular proliferation, and brisk mitotic activity.[4] On the other hand, criteria for classifying the mesenchymal population as an undifferentiated

"sarcoma" included cytologically anaplastic spindle cells surrounded by pericellular basal lamina, high mitotic activity, and briskly elevated MIB-1 labeling index. Although we did not feel this component fit into any of the individualized sarcoma entities acknowledged by the current WHO classification of soft tissue and bone tumors, expression of desmin and smooth muscle actin nevertheless indicated smooth muscular–related lineage.[14]

Although oligodendroglioma is common in dogs,[1,7,9] oligosarcoma has not been previously reported. In humans, differentiation of oligosarcoma from gliosarcoma has been suggested to directly impact on clinical decision making, because oligodendroglial differentiation tends to confer significant advantage with respect to both prognosis and adjuvant treatment options.[9–12,15–17] Clinical prospective studies would be necessary to evaluate any possible impact of oligodendroglial differentiation on the biologic behavior of biphasic glial tumors in dogs. Reports on human oligosarcomas[9–11,15,16] suggest that these tumors result from sarcomatous transformation of oligodendrogliomas, as they tend to occur in patients with a long history of clinical signs or upon tumor recurrence after surgical, medical, or radiation treatment. In contrast, the dog described in this report had a relatively short history and no history of treatment other than anti-inflammatory drugs.

Oligodendrogliomas typically present as single, fairly well-delineated, round, intra-axial masses arising in the cerebral hemispheres, sometimes extending to the subarachnoid space on MRI examination.[5–8] In the dog presented here, the intra-axial portion of the mass, which was predominated by the oligodendroglial population, exhibited features of a conventional anaplastic oligodendroglioma[2] including hypointensity in T1W sequences, hyperintensity in T2W sequences, presence of fluid-filled cavities with incomplete suppression in FLAIR images (interpreted as focal areas of necrosis or proteinaceous fluid accumulation), along with ring-like contrast enhancement. In contrast, a significant portion of the oligosarcoma moiety obliterated the subarachnoid space, extending from the temporal lobe into the caudal fossa. Here, the sarcomatous elements prevailed, and showed strong and homogeneous contrast enhancement. It is conceivable that these different MRI patterns within the oligosarcoma are related to the coexistence of both oligodendroglial and sarcomatous components.

In conclusion, oligosarcoma—although rare—should be considered in the differential diagnosis of canine CNS tumors. As MRI cannot be used to reliably differentiate oligosarcoma from other glial tumors, brain biopsy is essential for definitive diagnosis. The occurrence of oligosarcoma in dogs adds a novel facet to the histologic versatility of canine oligodendroglial tumors and emphasizes their phenotypical similarity to their human counterparts. Whether the analogy goes beyond a shared morphologic repertoire, eg, commonalities in molecular signatures, clinical behavior, and responsiveness to treatment, merits further investigation. Such insight will have the potential to directly benefit veterinary patients.

Footnotes

[a] Panorama 1.0T HFO; Philips Healthcare, DA Best, The Netherlands
[b] Propofol Fresenius 1%; Fresenius Kabi, Oberdorf, Switzerland
[c] Fentanyl–Curamed; Actavis, Regensdorf, Switzerland
[d] Anti Olig2, (AB9610) polyclonal; Millipore, Billerica, MA
[e] Dako, Glostrup, Denmark
[f] Smooth muscle actin clone 1A4; Sigma, St Louis, MO

Acknowledgments

Conflict of Interest Declaration: Authors disclose no conflict of interest.

Off-label Antimicrobial Declaration: Authors declare no off-label use of antimicrobials.

References

1. Snyder JM, Shofer FS, Van Winkle TJ, et al. Canine intracranial primary neoplasia: 173 cases (1986–2003). J Vet Intern Med 2006;20:669–675.

2. Meintjes RA. An overview of the physiology of pain for the veterinarian. Vet J 2012;192:344–348.

3. Driver CJ, Volk HA, Rusbridge C, et al. An update on the pathogenesis of syringomyelia secondary to Chiari-like malformations in dogs. Vet J 2013;198:551–559.

4. Louis DN, Ohgaki H, Wiestler OD, et al. The 2007 WHO classification of tumours of the central nervous system. Acta Neuropathol 2007;114:97–109.

5. Wisner ER, Dickinson PJ, Higgins RJ. Magnetic resonance imaging features of canine intracranial neoplasia. Vet Radiol Ultrasound 2011;52:S52–S61.

6. Wolff CA, Holmes SP, Young BD, et al. Magnetic resonance imaging for the differentiation of neoplastic, inflammatory, and cerebrovascular brain disease in dogs. J Vet Intern Med 2012;26:589–597.

7. Young BD, Levine JM, Porter BF, et al. Magnetic resonance imaging features of intracranial astrocytomas and oligodendrogliomas in dogs. Vet Radiol Ultrasound 2011;52:132–141.

8. Cervera V, Mai W, Vite CH, et al. Comparative magnetic resonance imaging findings between gliomas and presumed cerebrovascular accidents in dogs. Vet Radiol Ultrasound 2011;52:33–40.

9. Vajtai I, Vassella E, Hewer E, et al. Sarcomatous evolution of oligodendroglioma ("oligosarcoma"): Confirmatory report of an uncommon pattern of malignant progression in oligodendroglial tumors. Pathol Res Pract 2012;208:750–755.

10. Romero-Rojas A, Diaz-Perez JA, Ariza-Serrano LM, et al. Primary gliosarcoma of the brain: Radiologic and histopathologic features. Neuroradiol J 2013;26:639–648.

11. Rodriguez FJ, Scheithauer BW, Jenkins R, et al. Gliosarcoma arising in oligodendroglial tumors ("oligosarcoma"): A clinicopathologic study. Am J Surg Pathol 2007;31:351–362.

12. Hiniker A, Hagenkord JM, Powers MP, et al. Gliosarcoma arising from an oligodendroglioma (oligosarcoma). Clin Neuropathol 2013;32:165–170.

13. Rodriguez FJ, Scheithauer BW, Perry A, et al. Ependymal tumors with sarcomatous change ("ependymosarcoma"): A clinicopathologic and molecular cytogenetic study. Am J Surg Pathol 2008;32:699–709.

14. Fletcher CDM, Unni KK, Mertens F, eds. Pathology and Genetics of Tumours of Soft Tissue and Bone. Lyon: IARC Press; 2002.

15. Kanamori M, Kumabe T, Shibahara I, et al. Clinical and histological characteristics of recurrent oligodendroglial tumors: Comparison between primary and recurrent tumors in 18 cases. Brain Tumor Pathol 2013;30:151–159.

16. Weller M, Berger H, Hartmann C, et al. Combined 1p/19q loss in oligodendroglial tumors: Predictive or prognostic biomarker? Clin Cancer Res 2007;13:6933–6937.

17. Kaplan KJ, Perry A. Gliosarcoma with primitive neuroectodermal differentiation: Case report and review of the literature. Neurooncol 2007;83:313–318.